Modeling and Validation of Fluid Flow-Geomechanics of Mauddud Reservoir in Sabriya Field*

I. Hossam[1], P. Ashok[2], K. Rajive[2], J. Al-Kandari[2], M. Yaser[3], A. Mohamad-Hussein[3], K. Khaqan[3], D. Press[3], G. Xi[3], K. Lee[3], and C. Tan[3]

Search and Discovery Article #41052 (2012)**
Posted October 22, 2012

*Adapted from extended abstract prepared in conjunction with poster presentation at AAPG International Convention and Exhibition, Singapore, 16-19 September 2012, AAPG©2012

[1]Kuwait Oil Company (HDIbrahim@kockw.com)
[2]Kuwait Oil Company
[3]Schlumberger

Abstract

The combined process of reservoir injection and depletion results in changes in effective in-situ stresses, which may cause formation deformation and thus dynamic change of permeability in the reservoir. A 3D reservoir geomechanics modeling was conducted for the Mauddud reservoir in the Sabriya Field located in North Kuwait. A series of sensitivity analyses were carried out to examine the impact of permeability enhancement on well performance. The numerical results showed significant improvement of the reservoir production history match using coupled geomechanics. 3D mud weight cube was then constructed for field-scale drilling optimization. In addition, the impact of pore pressure change on fault stability was examined and wellbore stability analysis was performed for a planned well intersecting a fault.

3D Geomechanical Model Construction

A 3D geomechanical model was built based on the original reservoir model. The seismic horizons were used to define the geometry of the over-burden. Figure 1 shows the original geometry of the reservoir model and the seismic horizons for Sabriya Field.

Side-burdens were constructed on the sides of the reservoir. The under-burden was extended at the base of the model to help improve the aspect ratio and ensure a reasonable transfer of stress from boundaries to the reservoir and over-burden during the stress simulation. The interpreted fault planes from seismic data were incorporated into the 3D geomechanical model.

Figure 2 shows the position of the reservoir in relation to over-burden, side-burdens, and under-burden and the fault sticks for Sabriya Field.

Rock elastic and strength properties were defined using porosity correlations based on an extensive database, which included well data, in-situ measurements, and triaxial test data. The equivalent mechanical properties for faults were related to intact rock mechanical properties.

Pre-production Stress Modeling

Representative 3D pre-production stress state was obtained and validated against the stress state along five (5) wells. The comparison showed a good agreement between the 3D predicted and the 1D MEM (Mechanical Earth Model) stresses at the wells locations. Figure 3 shows the comparison between 3D stress distribution and 1D MEM stresses for a representative well. The computed initial stress state was representative of the in-situ condition and was used as initial condition for the fluid flow-geomechanical coupled modelling.

Coupled Fluid Flow-Geomechanical Modeling

Once the reservoir starts production, the stress state change and the effect of this change on potential geomechanics related issues such as fault stability, wellbore stability, and integrity of completions need to be re-assessed. Moreover, the changes in stresses cause the deformation of the reservoir rock that will modify its porosity and permeability, which in turn may change the production rate at the wells.

Coupling between fluid flow and the rock deformation in the reservoir and surrounding formations is very important to better understand the behaviour of the field (Heffer and Koutsabeloulis 1993; Koutsabeloulis and Hope 1998; Onaisi et al., 2002; Koutsabeloulis and Zhang 2009; Mohamad Hussein et al., 2010). It is necessary to introduce the geomechanical effects through a stress analysis solution and to implement a scheme that assures that governing laws of the flow simulation and the stress analysis are obeyed simultaneously in each time step.

Therefore, to fully understand these interactions, it was necessary to couple the geomechanical model with the fluid flow model, and ensure all relevant parameters were consistent between the two models.

The history matched fluid flow model was used as the base model for the coupled geomechanical analysis. Figure 4 shows the workflow for the fluid flow-geomechanical coupling approach. The fluid flow simulator computed the pressure distribution within the reservoir which was used as input into geomechanical simulator. The geomechanical simulator then computed the stress variables (stresses, strains, and displacements) which were subsequently used to compute an updated permeability. The permeability was updated in the subsequent fluid flow time step and pressures were computed based on the updated permeability. Such an approach shows the impact of geomechanics on the reservoir behaviour. Contrary to the conventional approach, the coupled geomechanics reservoir simulation approach enables permeability updating at each grid cell in the reservoir model with time and provides better control on the history match process and results.

The choice of permeability enhancement law is important in the hydro-mechanical coupling approach (Dutta et al., 2011). The law should reflect the material behaviour under different loading conditions. A two permeability updating technique was used to simulate:

- Permeability reduction resulting from reservoir elastic, volumetric and pore contraction deformations.
- Permeability increase due to plastic shearing which included dilation of shear bands.

The dynamic updating process enhanced the history matching capabilities of a solely fluid flow simulator. The total water production and total oil production were plotted for a number of wells. The comparisons between the predicted and observed data along a key well are shown in Figure 5. This comparison showed the impact of geomechanics on improved prediction of the behaviour of the well. The fluid flow-geomechanical model was more reliable in predicting the history of the well.

Comparisons between prediction and field history were also conducted. Figure 6 shows the comparison between predicted and field water production rate and total water production. These comparisons showed that fluid flow-geomechanical results using dynamic permeability updating improved the overall field predictions.

3D Mud Weight Cube

The stress state from fluid flow-geomechanical results was used to construct 3D mud weight cubes for the field. The mud weight cubes can be used to establish the width of the stable mud weight window based on the difference between the breakout mud weight limit and the breakdown mud weight limit (Figure 7). The mud weight cube is helpful for making decisions with regard to new well trajectories and well placements. It will provide general guidelines in regard to optimum wellbore direction for different formations and locations of the field.

Wellbore Stability Analysis

Wellbore stability analysis was performed on a planned well passing through a fault. A 3D well-centric numerical model was created by inserting the planned well trajectory into the 3D geomechanical model as shown in Figure 8 (left). Wellbore stability predictions were made for the chosen mud weight and wellbore deformation was predicted along the planned trajectory. This figure (Figure 8 right) illustrates the distribution of plastic shear strains occurring in a small region around the borehole. The magnitude of plastic shear strain is very small (~0.01%) which is unlikely to cause any wellbore stability issues, suggesting that wellbore is stable for the given mud weight.

Fault Stability Analysis

Normal and shear stresses on fault planes continue to change as in-situ effective stresses change with pore pressure change during injection and production. By analyzing the effective normal and shear stresses and associated plastic shear strain on the fault planes, faults stability analysis was performed.

Figure 9 (left) shows the distribution of plastic shear strain along the faults at Feb 2010. The largest plastic shear strains were in regions where the injection and depletion were maximum. Due to injection and depletion, the rock tends generally to expand and compact, respectively and thus generated displacement along the fault surface. This displacement results in induced shearing and release of plastic energy. The plastic shear strains represented an indicator of the potential of fault reactivation. Material within the faults experienced a change in state of stress during depletion and injection. The state of stress can be defined by normal stress and shear stress in the fault.

Figure 9 (right) shows the stress state of cells within fault FSA30_S_11 at 2010 (green data symbols) and 2040 (blue data symbols). Each point represents the stress state for a fault cell. Points below the failure line indicate zone of stability. Points along the failure line represent cells with failure stress state and potential to contribute to fault reactivation. This fault is located within regions that experienced injection. Due to injection, effective stresses are reduced and thus the points, in general, shifted to the left and closer to the failure line. The analysis helps understand critical stressed nature of the faults and can be used to address practical field problems such as wellbore and casing integrity, premature water cut, and anomalous production behaviour of wells in the proximity of fault.

Conclusions

Water and oil productions and well pressure were examined at key wells. The results from coupled geomechanical simulations showed significant improvements of predicted well pressure, and water and oil productions when compared with measured data. The overall field behavior also showed improvement with respect to water cut as well as water and oil production. The comparison of predictions with field measured data indicate that water production predictions were improved for 65% of selected key wells and bottomhole pressure predictions were improved for 93% of the wells, while oil production predictions were more or less the same as the original ECLIPSE model.

3D mud weight cubes were computed and used to establish the width of the stable mud weight window based on the difference between the breakout mud weight and the breakdown mud weight limit for a combination of well azimuths and inclinations. The output provided guidelines on optimum wellbore direction for different formations and locations of the field.

Wellbore stability for the planned well using 3D near-wellbore numerical model showed negligible yielding at the wellbore wall for the proposed mud weight programme, suggesting that wellbore is stable during drilling.

Fault stability analysis of a fault intersected by the planned well showed that there was minimal potential of drilling risk for the well.

Acknowledgments

The authors wish to thank Kuwait Oil Company and Schlumberger for permission to publish this work. The conclusions and views presented in this paper are the authors' and do not necessarily reflect the view of their organizations.

References

Dutta, D., C.V.G. Nair, X. Zhang, A. Mohamad-Hussein, M. Yaser, D. Press, N.F. Al-Khalifa, E.H.E. Faldi, and N. Koutsabeloulis, 2011, A 3D Coupled Reservoir Geomechanics Study for Pressure, Water Production, and Oil Production Simulation: Application in Umm-Gudair Field, West Kuwait: SPE 147943 Paper presented at SPE Reservoir Characterization and Simulation Conference and Exhibition in Abu Dhabi, UAE.

Heffer, K.J., and N.C. Koutsabeloulis, 1993, Stress effects on reservoir flow—numerical modeling used to reproduce field data: New Developments in Improved Oil Recovery, Geological Society Special Publication, no. 84.

Hussein, M.A., J. Minton, K. Rawnsley, L. Qiuguo, X. Zhang, and K. Koutsabeloulis, 2010, Coupled Reservoir Geomechanical Modeling of a Thermal Gas-Oil-Gravity-Drainage Project: SPE 127822 Paper presented at SPE EOR Conference at Oil & Gas West Asia held in Muscat, Oman, DOI: 10.2118/127822-MS.

Koutsabeloulis, N., and X. Zhang, 2009, 3D Reservoir Geomechanical Modeling in Oil/Gas Field Production: SPE 126095 Paper presented at the SPE Saudi Arabia Section Technical Symposium and Exhibition held in Alkhobar, Saudi Arabia, DOI: 10.2118/126095-MS.

Koutsabeloulis, N.C., and S.A. Hope, 1998, Coupled Stress/Fluid/Thermal Multi-Phase Reservoir Simulation Studies Incorporating Rock Mechanics: SPE/ISRM 47393 Paper presented at the SPE Annual Technical Conference and Exhibition, Trondheim, Norway, DOI: 10.2118/47393-MS.

Onaisi, A., P. Samier, N. Koutsabeloulis, and P. Longuemare, 2002, Management of Stress Sensitive Reservoirs Using Two Coupled Stress-Reservoir Simulation Tools: ECL2VIS and ATH2VIS: SPE 78512 Paper presented at the 10th Abu Dhabi International Petroleum Exhibition and Conference, DOI: 10.2118/78512-MS.

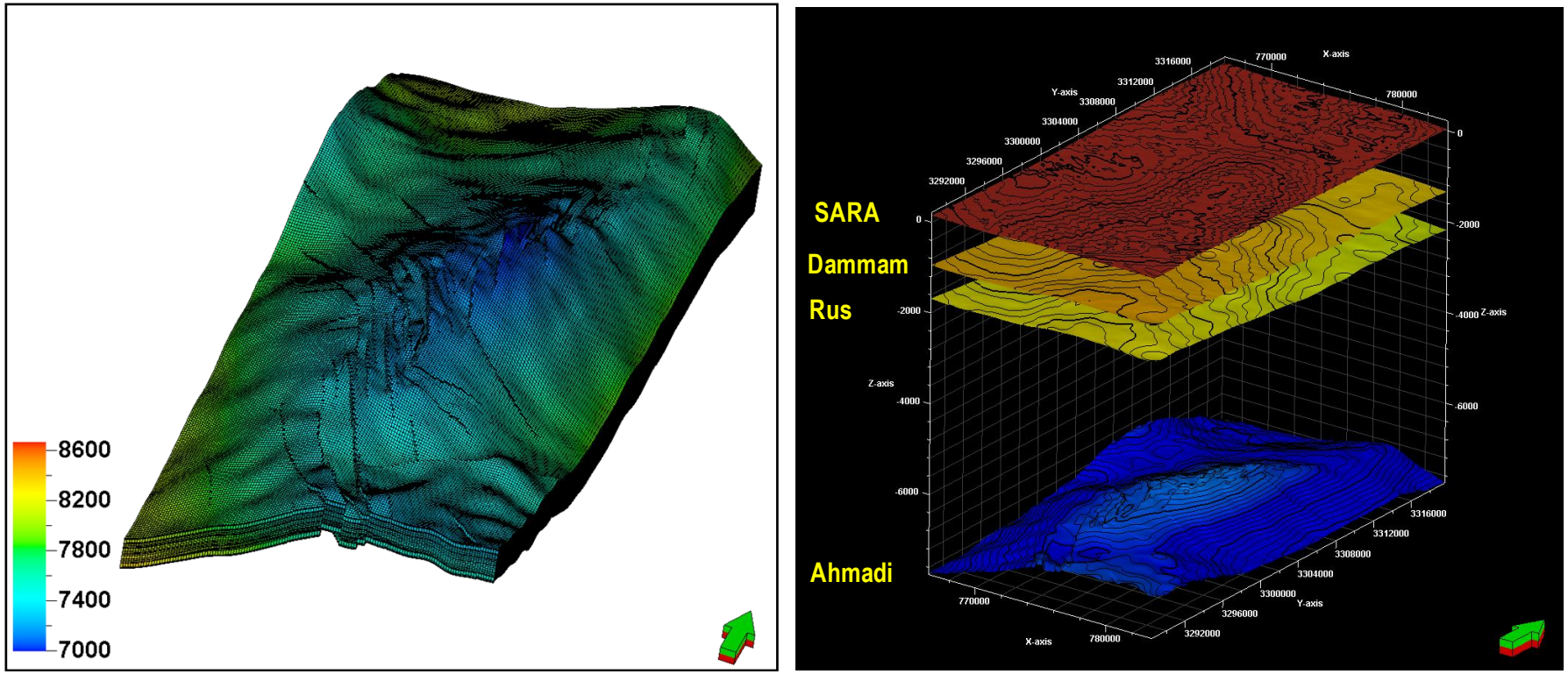

Figure 1. Original reservoir model (depth in ft) (left) and seismic horizons (right).

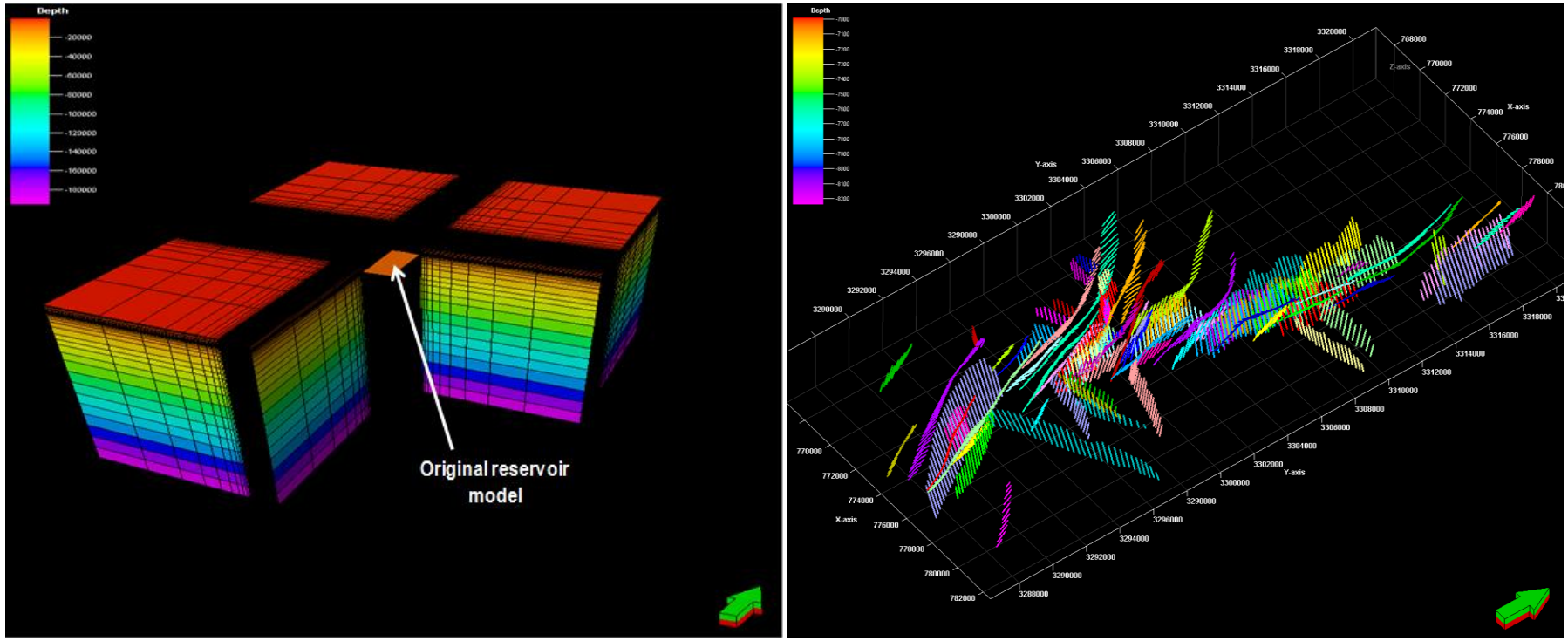

Figure 2. 3D geomechanical model geometry with ¼ cut out illustrating the position of the reservoir (ft) (left) and fault sticks (right).

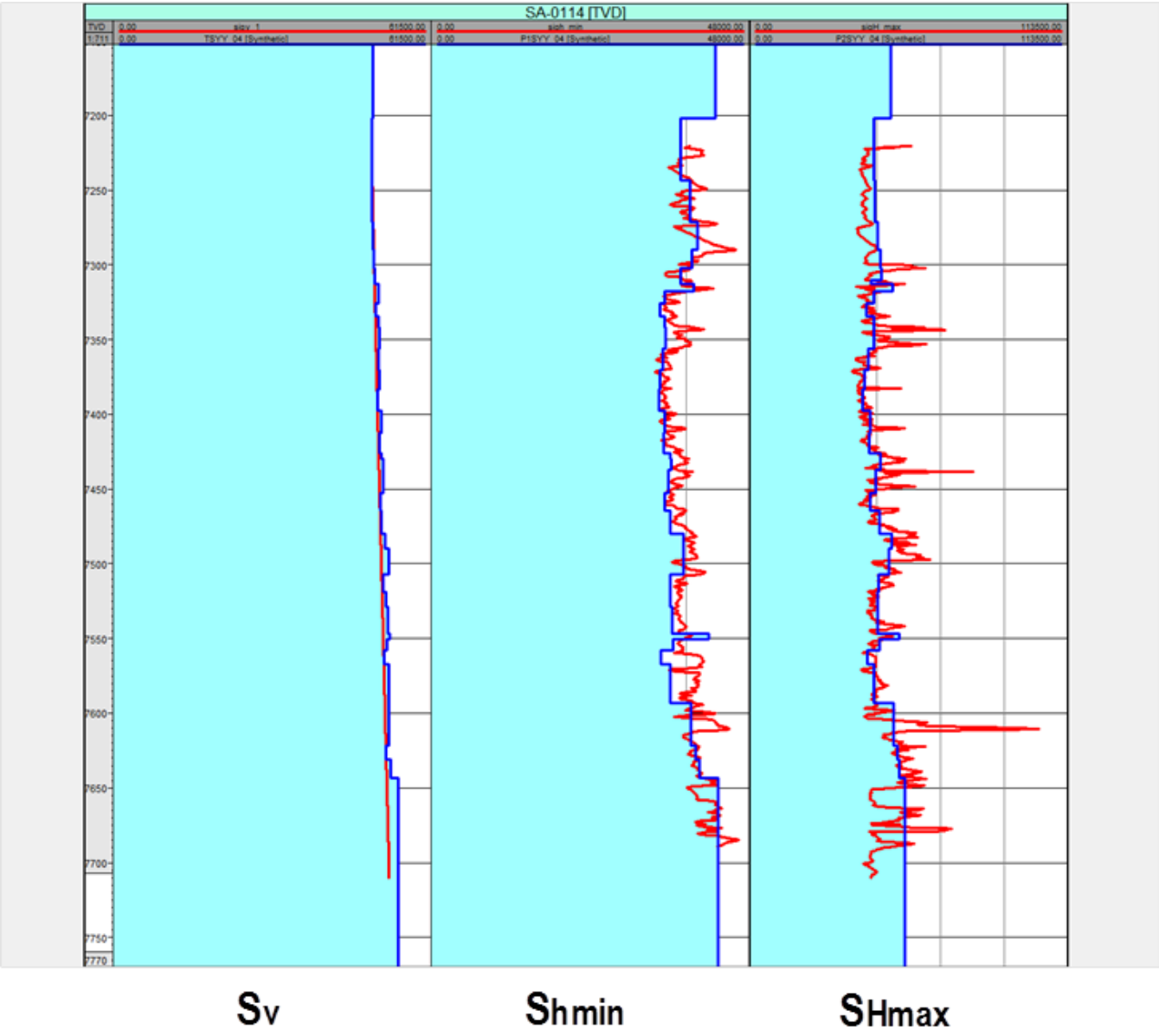

Figure 3. Comparison between 3D (blue) and 1D MEM (red) stresses (psi) in a representative well.

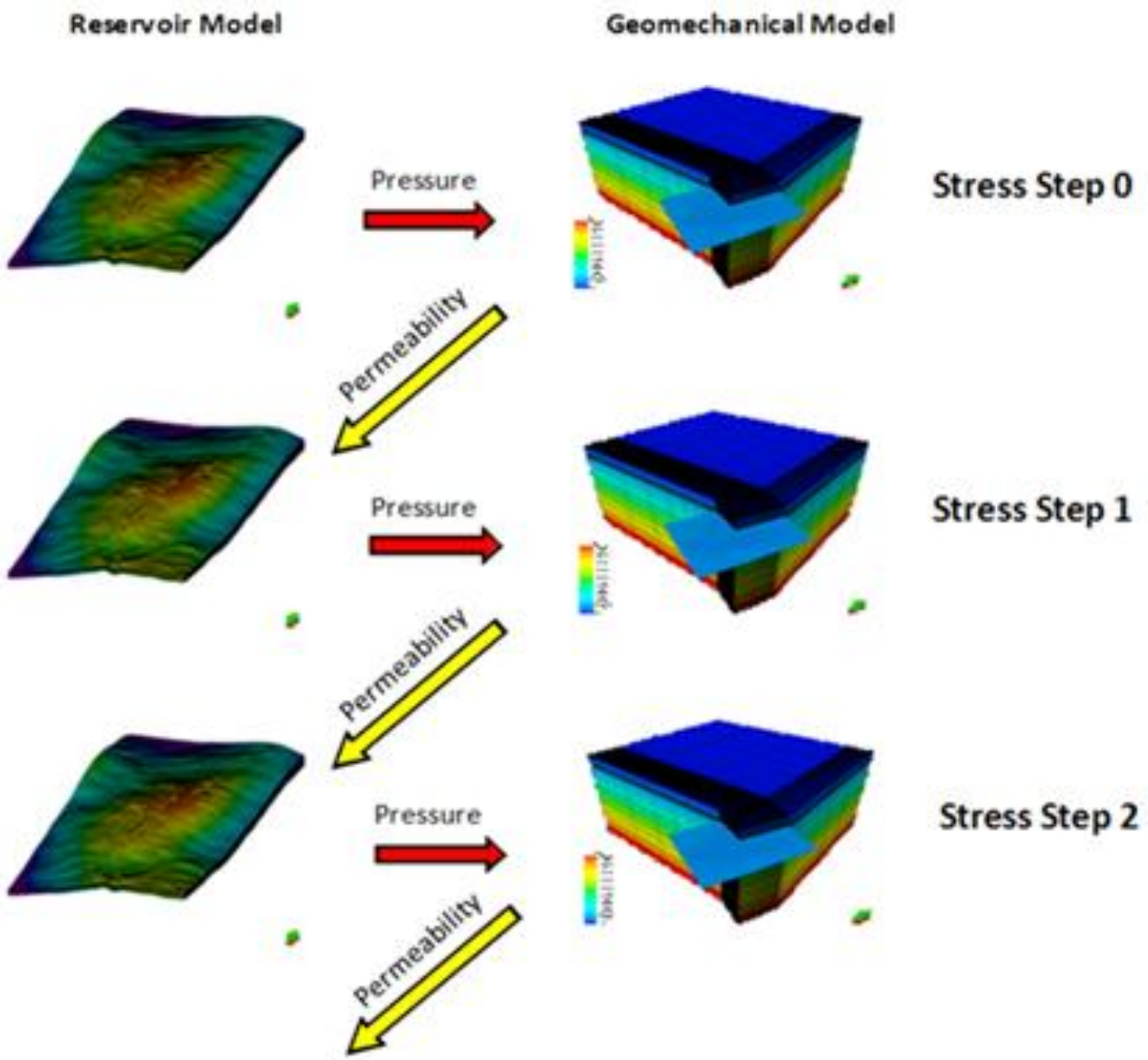

Figure 4. Fluid flow-geomechanical coupling workflow.

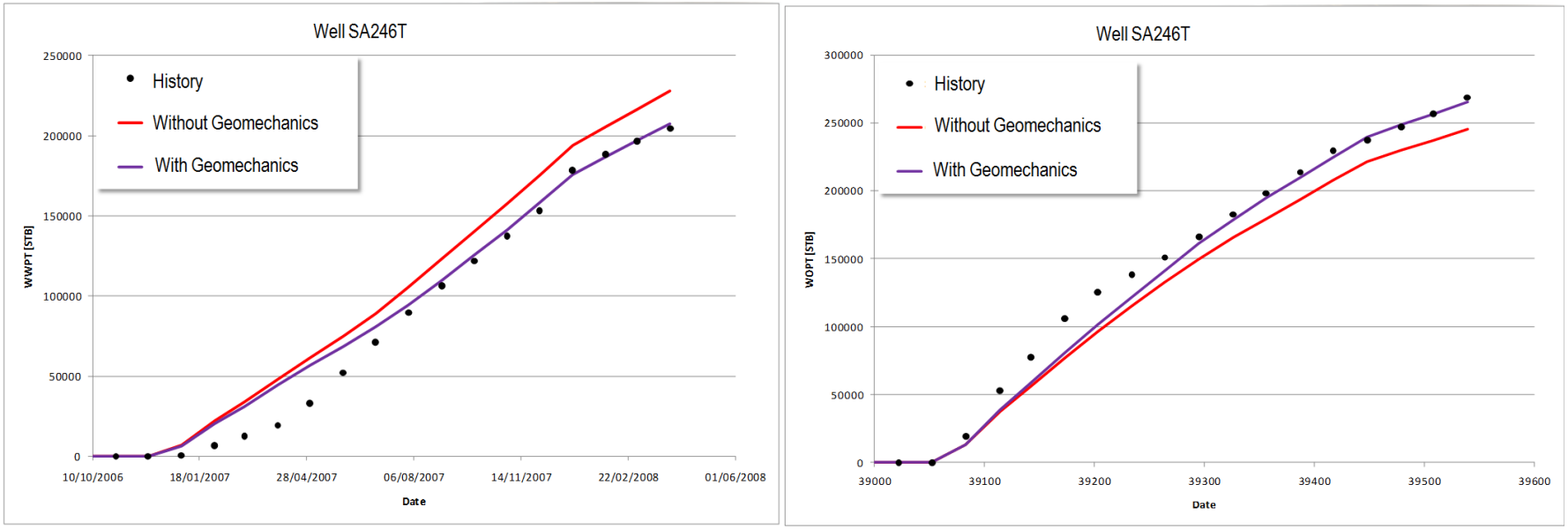

Figure 5. Comparison between predicted and observed total water production (left) and total oil production (right) in well SA246T.

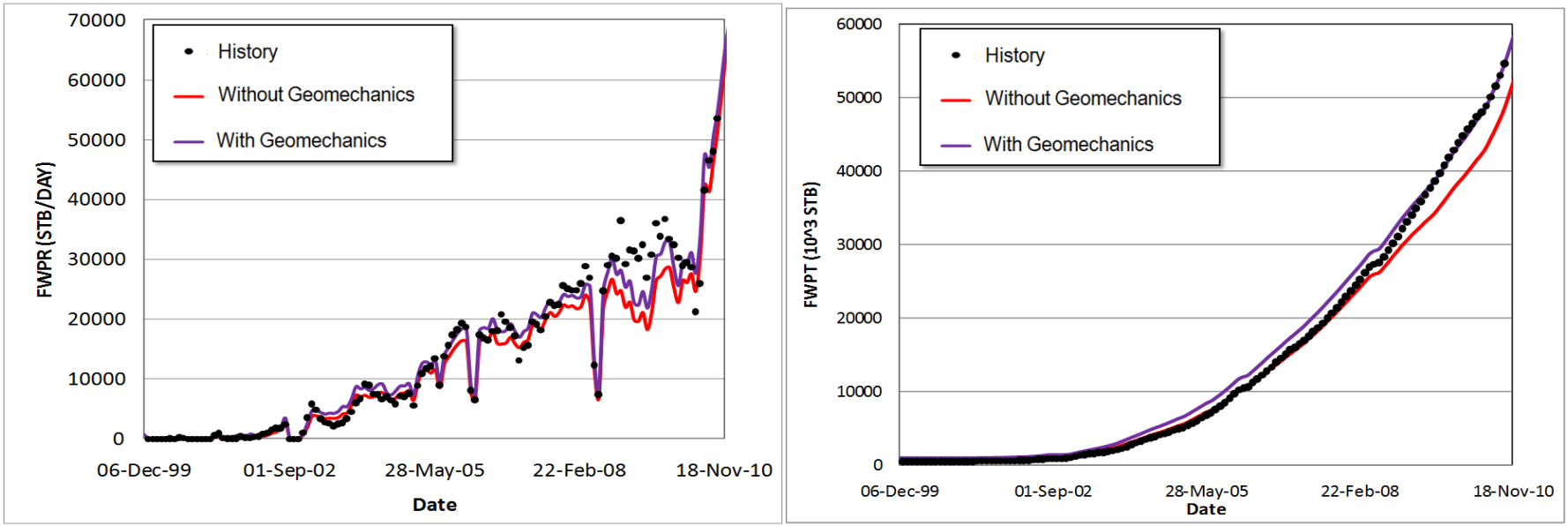

Figure 6. Comparison between predicted and observed field water production rate (left) and total field water production (right).

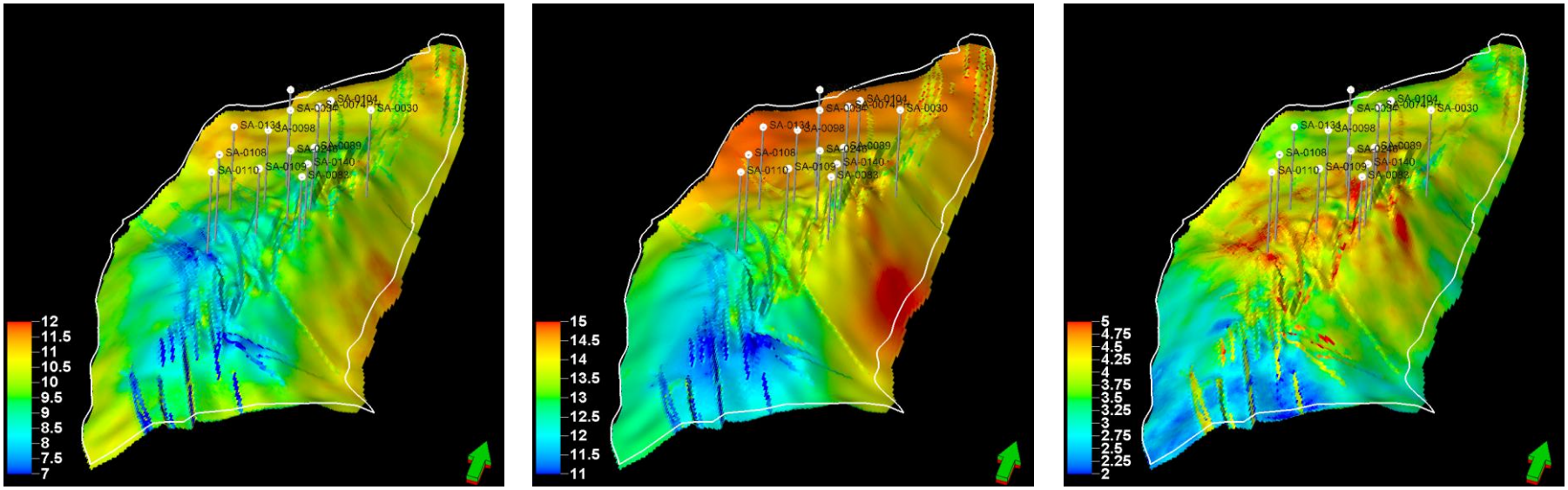

Figure 7. Distribution of breakout mud weight (ppg) (left), break down mud weight (ppg) (middle) and stable mud weight window (ppg) (right) within a representative reservoir layer.

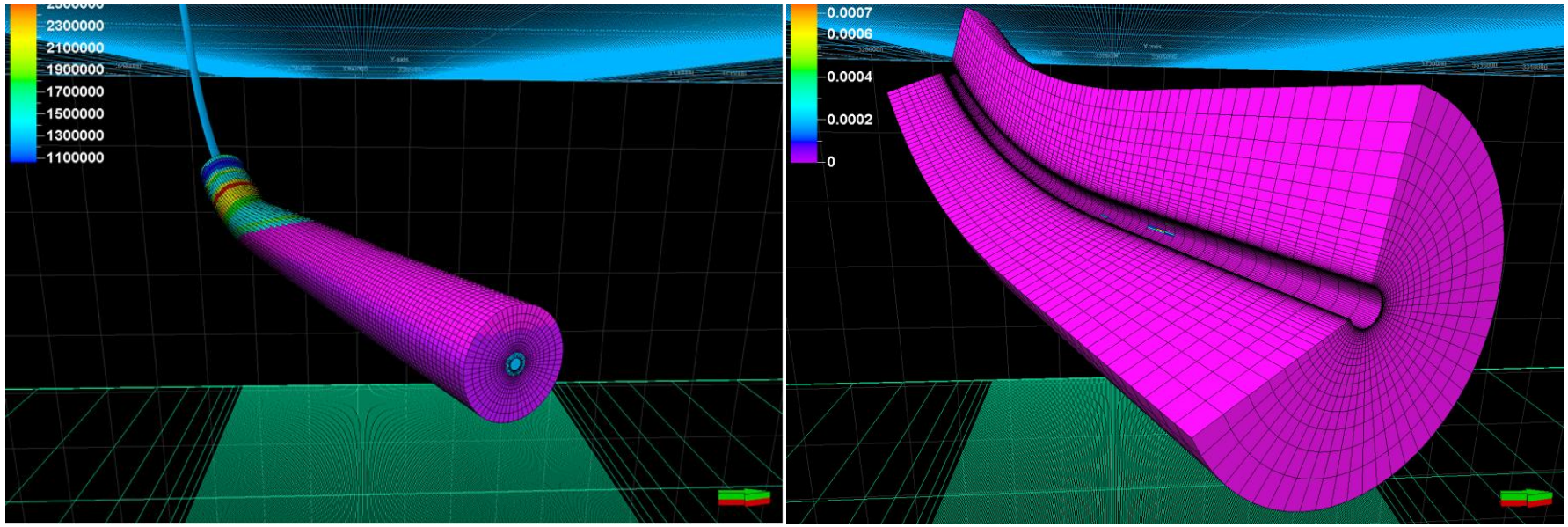

Figure 8. Distribution of Young's modulus (psi) in the well-centric model (left) and distribution of plastic shear strain after well excavation (right).

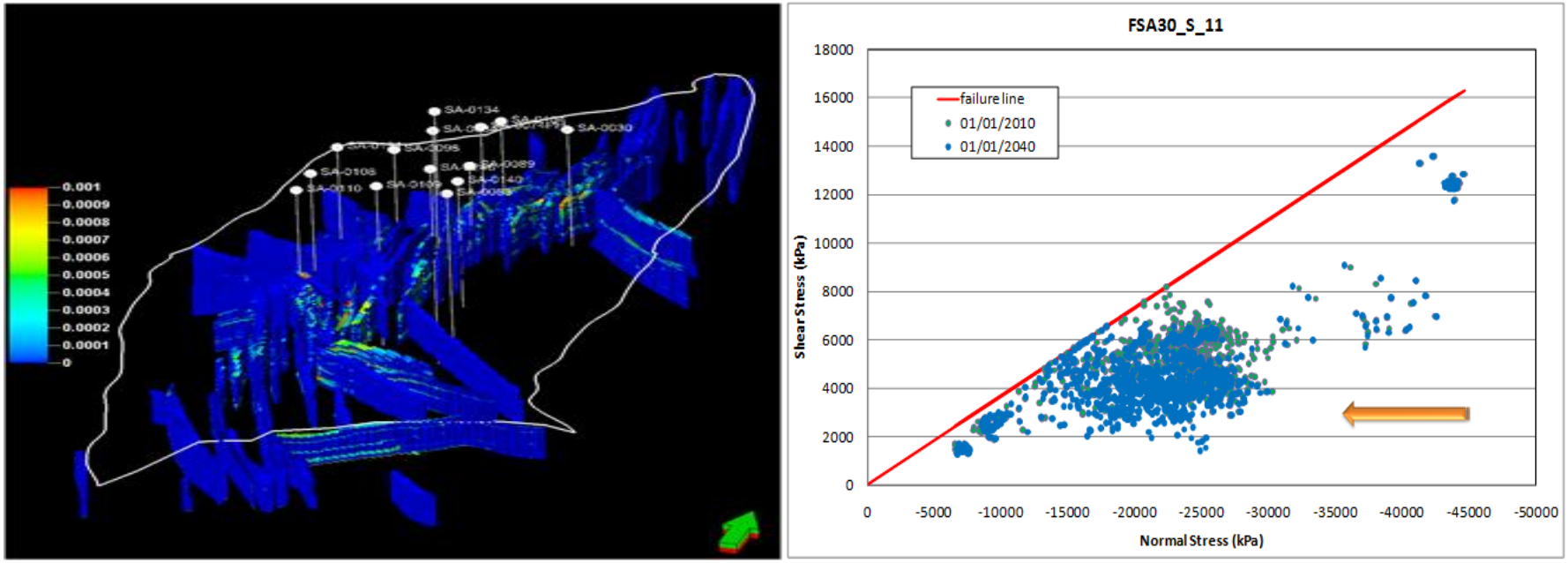

Figure 9. Distribution of plastic shear strain along faults at 01/02/2010 (left) and stress state of fault cells in Fault FSA30_S_11 at 01/02/2010 and 01/01/2040.